Preparation of Microporous Silica Gel by Sol–Gel Process in the Presence of Ethylene Glycol Oligomers

Ryoji Takahashi,* Satoshi Sato, Toshiaki Sodesawa, Masanori Suzuki, and Katsuyuki Ogura

Department of Materials Technology, Faculty of Engineering, Chiba University, Yayoi, Inage, Chiba 263-8522

(Received September 13, 1999)

A microporous silica gel was prepared by a sol–gel process in the presence of ethylene glycol (EG) and its oligomers (oligoEG), and the pore formation process was investigated by using NMR and TG-DTA. The micropore volume changed with the polymerization degree of oligoEG, and showed a minimum at the trimer of EG. An attractive interaction between silanol and organic additives plays a key role in micropore formation: the interaction inhibits the bond formation of Si–O–Si during drying and heating, and heterogeneous domains which convert into micropore are formed after the combustion of additives. There are two kinds of interaction: one is ester (Si–OR) bond formation of a silanol with an end hydroxy group of additives; the other is hydrogen bonding between a silanol and an ether oxygen of additives. The former interaction is significant for EG. With increasing length of oligoEG, however, the former interaction rapidly disappears, while the latter becomes stronger. Because of a minimum in the combination of these interactions, the minimal volume of the micropore is observed.

Porous materials with controlled pore structures have many applications, such as filters, adsorbates, catalysts, and catalyst supports. Depending on the size, pores are classified into micropore, mesopore, and macropore, whose pore diameters (d) are in the ranges of $d < 2$ nm, $2 < d < 50$ nm, and $d > 50$ nm, respectively. Microporous materials have been proposed for such applications as gas separation,[1] molecular-recognition in catalysis,[2–4] and humidity self-control.[5] For example, Okada et al. have prepared a powder of γ-alumina with pore diameter of ca. 2 nm by a selective leaching method,[6] and tested the humidity-control ability of its fired body.[5]

Recently, a sol–gel process has attracted much interest as a method to prepare porous inorganic materials with different structures. Several research groups have prepared microporous silica membranes by a sol–gel method using silicon alkoxide modified with an organic functional group for a gas-separation film at high temperature.[7–10] Micropore-tailoring of silica gel in sol–gel process has also been performed by the addition of organic compounds.[11–14] In these preparations of microporous silica gel through the sol–gel route, the organic ligands and additives have been considered to disperse at molecular level in the gel matrix, and to work as templates for pore formation.[10,13] Generally, phase separation occurs when organic additives which show a repulsive interaction with the silica-gel network, i.e. make the free energy of mixing positive, are used.[15,16] For the purpose of dispersing the additives homogeneously in the silica-gel matrix to work as templates, some attractive interactions are needed between the silica gel and the additives.

Ethylene glycol (EG)[11,12] and poly(ethylene glycol) (PEG)[13] have been reported to work well as additives for micropore formation. However, how they work for pore formation has not yet been clarified. Nakanishi et al. have reported in an investigation of phase separation in the silica-poly(ethylene oxide) (PEO) system that a strong attractive interaction arises between the silica gel and PEO.[17,18] A similar interaction must arise between silica and the polymer with a shorter oxyethylene chain, such as oligo(ethylene glycol) (oligoEG). In this paper, we discuss the interaction between oligoEG and silica in xerogel, and clarify the mechanism of pore formation.

Experimental

Sample Preparation. Tetraethyl orthosilicate (TEOS, Shinetsu Co.) was used as a source of silica. As organic additives, we used ethylene glycol (EG) and its oligomers, such as diethylene glycol (DEG), triethylene glycol (TEG) and PEG with average molecular weights of 300 (HEG) and 3000 (PEG3000). The average polymerization degree (n) of HEG and PEG3000 were ca. 6.4 and 68, respectively. All of the additives were supplied by Wako Chemical Ltd. Nitric acid and ammonia aqueous solutions were used as catalysts for hydrolysis and condensation of TEOS.

The sol–gel reaction was carried out by a two-step hydrolysis method.[13] In the first step, a 1 mol dm^{-3} nitric acid aqueous solution was added into a mixture of TEOS and ethanol (EtOH), dissolving each oligoEG under stirring at 20 °C. The molar ratio was adjusted to be TEOS : H_2O : EtOH = 1 : 1 : 4. After being stirred for 1 h, additional EtOH and a 1 mol dm^{-3} nitric acid aqueous solution were added (second step). The final composition was set at TEOS : H_2O : EtOH = 1 : R : 6, where R was varied from 2 to 12. The amount of oligoEG (x) was calculated as the weight ratio of oligoEG to SiO_2. The final pH of the solution was ca. 0.2. To clarify the effect of the solution pH, a 1 mol dm^{-3} ammonia aqueous solution and distilled water were used in the second step instead of a nitric acid aqueous solution. The typical compositions are listed in Table 1. The solution was kept in an open container at 20 °C for 2—3 d for gelation, and was dried at 50 °C for 3 d. The dried

Table 1. Typical Starting Compositions

Parameter	TEOS[a)]	H_2O[a)]	EtOH[a)]	PEG/SiO_2[b)]	Comments
PEG content	1	4	6	x	x = 0.37—1.48 for PEG3000
H_2O content	1	R	6	1.48	R = 2—12 for PEG3000
Oligomer	1	2.2	6	1.48	EG, DEG, TEG, HEG, and PEG3000
pH	1	2.2	6	1.48	pH = 0, 2, 7 for EG, TEG, PEG3000

a) Molar contents. b) Weight ratios.

sample was heated at 500 °C for 2 h with a heating rate of 100 K h^{-1} after crushing the sample into powder.

Characterization. Nitrogen-adsorption isotherm for each calcined sample was measured using a volumetric apparatus at −196 °C. Samples were degassed at 300 °C for 60 min under a reduced pressure of 1.3 Pa prior to each measurement. Because all of the isotherms were of the Langmuir type,[19] the *t*-plot method,[20] where adsorbed volume was plotted against average thickness (t) of multi-layer adsorption, was used to analyze the isotherm; also, the pore structure of samples with different preparation conditions was evaluated in terms of micropore volume. Total pore volume was also calculated from the volume of N_2 adsorbed at $P/P_0 \approx 0.95$. Thermal gravimetry and differential thermal analysis measurements (TG-DTA; Mac Science Co., WS002) were carried out in air flow at a heating rate of 10 K min^{-1} for samples dried at 50 °C to observe the decomposition behavior of the organic components.

To clarify the interaction between silica network and organic compounds, ^{29}Si and ^{13}C magic-angle spinning (MAS) NMR spectra for samples dried at 50 °C were measured on a Bruker DPX300 spectrometer operating under a static magnetic field of 7 T. A MAS speed of 4000 Hz was adopted. The radio frequencies of 59.6 MHz and 75.4 MHz were used for detecting ^{29}Si and ^{13}C resonances, respectively, and 300 MHz for ^1H decoupling. Pulse sequences with high-power ^1H decoupling (HPDEC) were used to assure quantitative information; 256 and 128 FID signals were accumulated with 30 and 90° pulse and a recycle time of 100 and 10 s for the ^{29}Si and ^{13}C NMR measurements, respectively. As a comparison, pulse sequences of ^1H-to-^{13}C cross polarization (CP) were also used for ^{13}C detection with a CP contact time of 1 ms. The chemical shifts of ^{29}Si and ^{13}C relative to tetramethylsilane (TMS) were determined by using peaks at 1.53 ppm of sodium 3-(trimethylsilyl)propane-1-sulfonate (DSS) and at 176.46 ppm of carboxyl carbon in glycine as external references, respectively. Small-angle X-ray scattering (SAXS) measurements were performed to observe the structure of dried samples. The details of the measurements were reported elsewhere.[21] Because powdering had generated strong scattering from a fractured surface in the sample, a thin plate of the sample was used.

Results

Figure 1 shows changes in the N_2 adsorption isotherm of silica gel prepared at R = 4 with various PEG3000 amounts (x). All of the samples showed Langmuir-type isotherms, suggesting the existence of micropores. Although the specific surface area of the samples can be mathematically calculated either by a BET method,[22] developed to calculate specific surface area for multi-layer adsorption on non-porous surface, or by a Langmuir plot for mono layer adsorption[19] (for example, 549 $m^2 g^{-1}$ by BET and 844 $m^2 g^{-1}$ by Langmuir for sample with x = 1.48), the calculated values have no physical meaning due to micropore

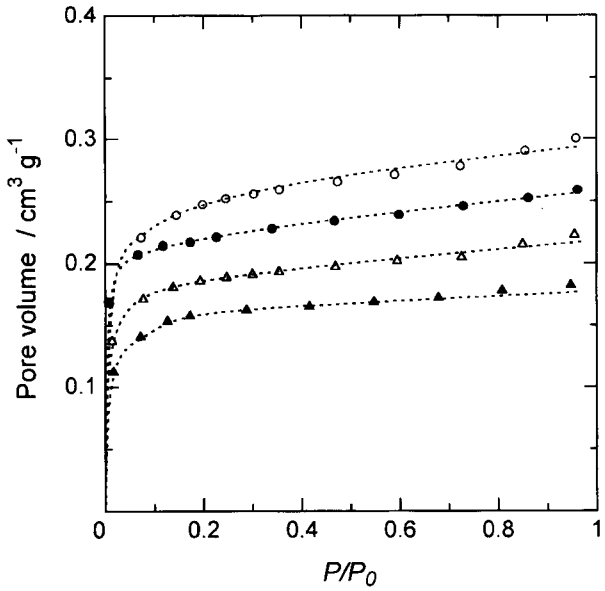

Fig. 1. N_2 isotherms for the calcined gel samples with various PEG3000 amount. The samples were prepared with composition of "PEG content" in Table 1. Weight ratio of PEG3000/SiO_2 were ○: 1.48, ●: 1.11, △: 0.74, ▲: 0.37.

condensation. Furthermore, we could not utilize methods, such as Barrett–Joyner–Halenda,[23] Cranston–Inkley,[24] and Dollimore–Heal,[25] to obtain the pore-size distribution, because these methods were proposed for pores larger than 2 nm in diameter, while our samples had pores smaller than 2 nm. To obtain the pore-size distribution in the micropore range, MP[26] and Horvath–Kawazoe[27] methods have been derived. However, we could not obtain a sufficient number of data points at a lower relative pressure to analyze the isotherm by these methods, because of a limitation in the efficiency of our apparatus. Therefore, we analyzed the isotherms by the *t*-plot method. Figure 2 shows variations of the micropore volume as well as the total pore volume with x, which were calculated from the isotherms in Fig. 1. Both the micropore volume and total one were 0 $cm^3 g^{-1}$ for a silica gel prepared without adding PEG3000. They increased steeply upon adding a small amount of PEG3000, and then gradually increased with increasing PEG3000 content. Figure 3 shows changes in the pore volumes of gels with the ratio of H_2O/TEOS (R) at x = 1.48. Although the volumes increased with an increase in R, the increase in volume was relatively small.

Figure 4 shows variations in the micropore and the total pore volumes with an average polymerization degree (n) of

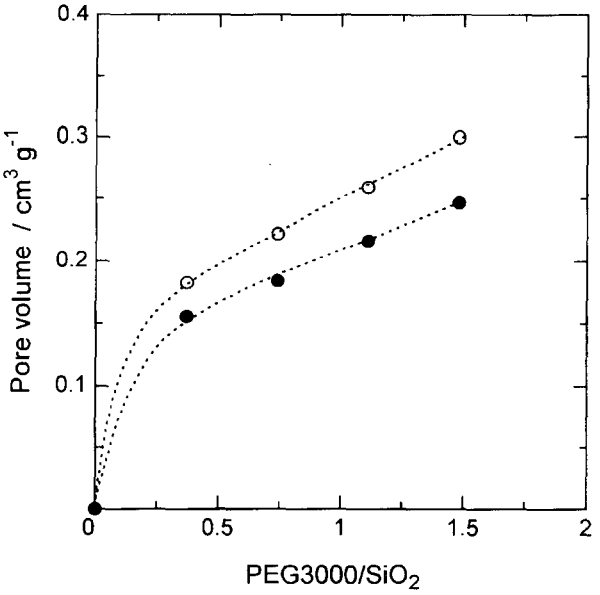

Fig. 2. Changes in micro (●) and total (○) pore volumes with PEG3000/SiO_2 ratio, which were calculated from the isotherms in Fig. 1.

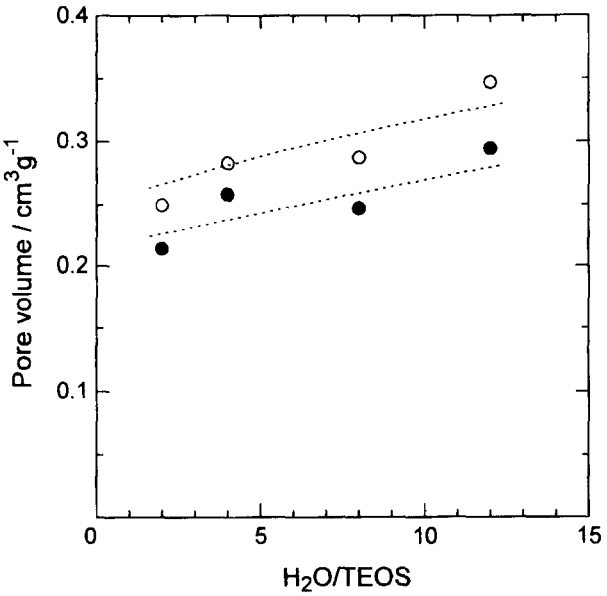

Fig. 3. Changes of micro (●) and total (○) pore volumes with H_2O/TEOS ratio for the calcined gel samples prepared with composition of "H_2O content" in Table 1.

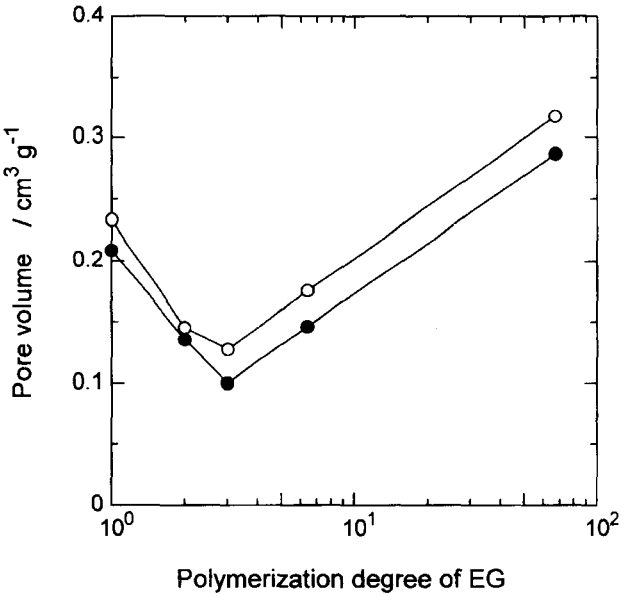

Fig. 4. Changes in micro (●) and total (○) pore volumes of calcined gel samples with polymerization degree of incorporated EG oligomers. The samples were prepared with composition of "oligomer" in Table 1.

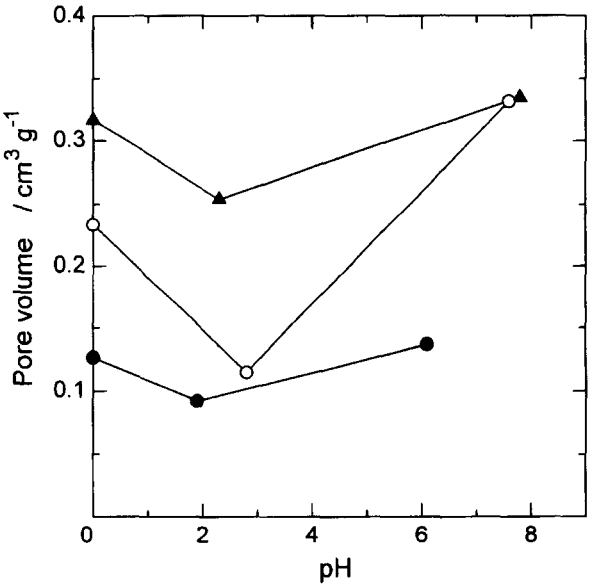

Fig. 5. Changes in micropore volume of calcined gel samples with pH for ▲: PEG3000, ●: TEG, ○: EG. The samples were prepared with composition of "pH" in Table 1.

added oligoEG. No linear correlation was observed between the pore volume and n. Both micro and total pore volumes passed minima at n = 3, i.e. at TEG. Figure 5 shows effect of the pH of the reacting solution on the micropore volume for the EG-, TEG-, and PEG3000-containing systems. Langmuir-type isotherms were also obtained when the pH of the solution was varied. The micropore volume showed a minimum at ca. pH = 2 for all samples. Especially in the EG sample, the micropore volume decreased greatly at pH = 2.

Figures 6 and 7 show DTA and TG profiles of dried samples containing oligoEG, respectively. The weight loss at a temperature of < 100 °C, accompanied by an endothermic peak, which was attributed to elimination of adsorbed water, was observed for all samples. The weight loss between 100 and 200 °C was also observed for the EG-, DEG-, and TEG-silica samples. Because the endothermic weight loss was shifted to the higher temperature side with an increase in n (Fig. 7), they would be attributed to the vaporization of free EG or its oligomers. Exothermic elimination of organic compounds was observed at the temperature range between 200 and 300 °C. The peak position shifted to the lower temperature side with an increase in n, from 290 °C for EG to

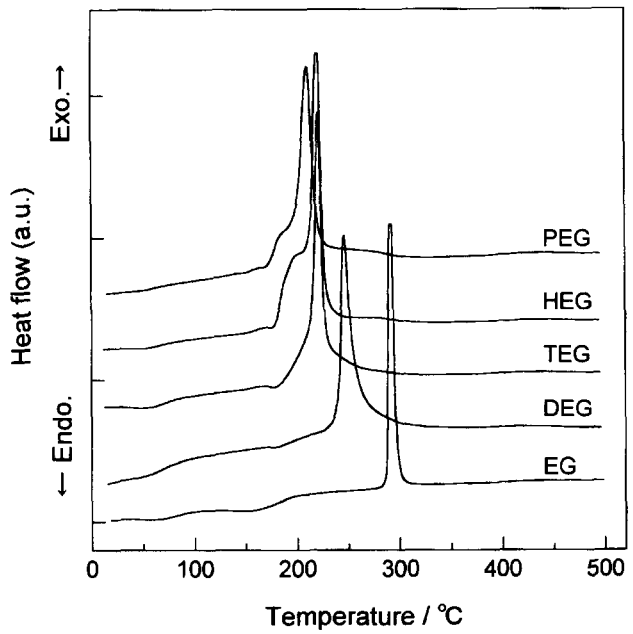

Fig. 6. DTA profiles of dried silica gels containing EG oligomers.

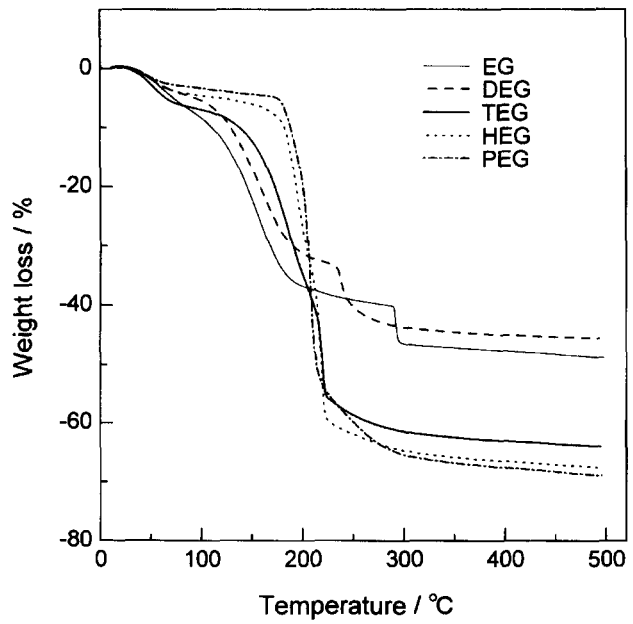

Fig. 7. TG profiles of dried silica gels containing EG oligomers.

210 °C for PEG3000 (Fig. 6), and the amount of additives eliminated exothermically increased with an increase in n. The overall weight loss up to 500 °C was 60—70 % for TEG-, HEG-, and PEG3000-silica, while it was 45% for EG- and DEG-silica. If we ignore the weight loss at < 100 °C, the ratio of the weight loss to the retained weight agrees well with that of additives/SiO_2 in the starting composition for HEG- and PEG3000-silica.

Figure 8 shows ^{29}Si NMR spectra for samples dried at 50 °C. In the spectra, 3 peaks were observed for all samples at -92, -101, and -111 ppm assigned to Q^2, Q^3, and Q^4, respectively.[28] Here, the symbol Q^n corresponds to a Si with

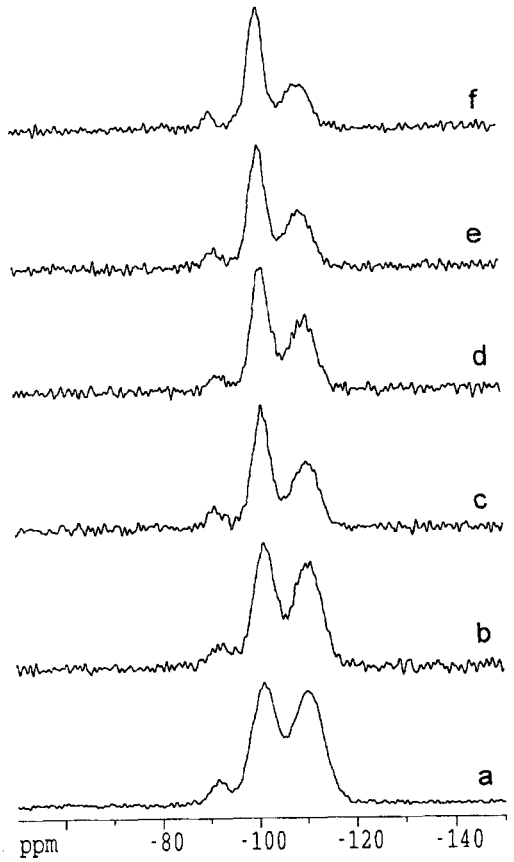

Fig. 8. ^{29}Si MAS NMR spectra of dried silica gels prepared (a) without organic additives, (b) with EG, (c) DEG, (d) TEG, (e) HEG, (f) PEG3000.

the formula $Si(OSi)_n(OR)_{4-n}$, where R is H or CH_2CH_3. For all samples, Q^3 is highest among these peaks, and proportion of Q^2 is small. Then, we can see a difference in the ratio of Q^4/Q^3 among the samples. The proportions of each peak area in Fig. 8 are summarized in Table 2. The ratio of Q^4/Q^3 decreased with an increase in n, whereas little difference was observed between EG-silica and silica prepared without additives. Namely, the condensation degree of silica in dried samples decreased with increasing n. Figure 9 shows ^{29}Si NMR spectra for typical calcined samples. After calcination, all of the samples had only Q^4, and no significant difference in the spectra was observed among the samples.

Figure 10 shows ^{13}C NMR spectra of dried silica gel containing PEG3000 together with that of pure PEG3000. Pure PEG3000 showed a broad peak centered around 70—73 ppm

Table 2. Fractions of Each Si Species in ^{29}Si NMR Spectra of Dried Samples

Sample	Q^2	Q^3	Q^4
Silica (without additives)	0.06	0.46	0.48
EG–silica	0.07	0.47	0.46
DEG–silica	0.07	0.53	0.4
TEG–silica	0.06	0.55	0.39
HEG–silica	0.06	0.57	0.37
PEG3000–silica	0.06	0.6	0.33

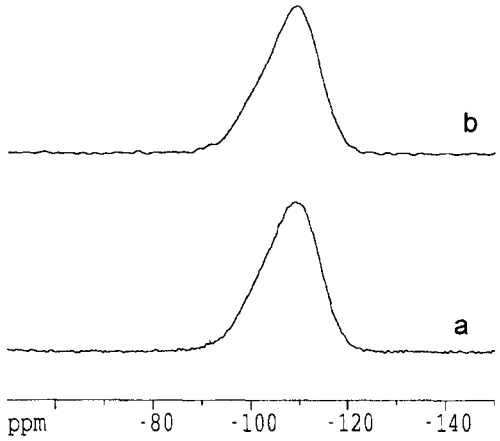

Fig. 9. ^{29}Si MAS NMR spectra of silica gels heated at 500 °C prepared (a) without organic additives, (b) with PEG3000.

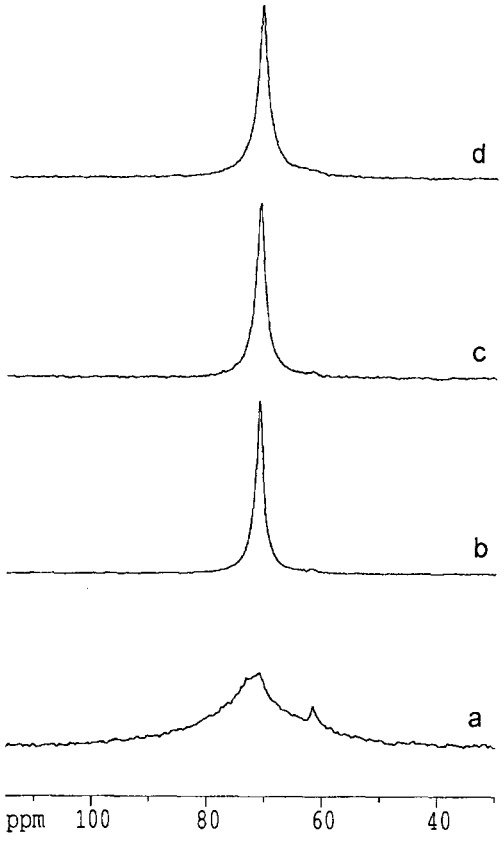

Fig. 10. ^{13}C MAS NMR spectra for (a) pure PEG3000 by HPDEC, (b) PEG3000–silica dried at 50 °C by HPDEC, (c) by CP, (d) dried at 80 °C by HPDEC.

(a). On the other hand, PEG3000-silica showed a sharper peak at 70.7 ppm (b). The spectra hardly changed with different pulse programs (b and c). At an elevated temperature of 80 °C, the resonance peak became somewhat broader than that at 50 °C. Figure 11 shows ^{13}C NMR spectra of dried silica gel containing EG together with that of pure EG. A resonance at 63.8 ppm, assigned to methylene carbon, was observed for pure EG (a). A similar spectrum was obtained for gel dried at 50 °C when the pulse sequence of HPDEC

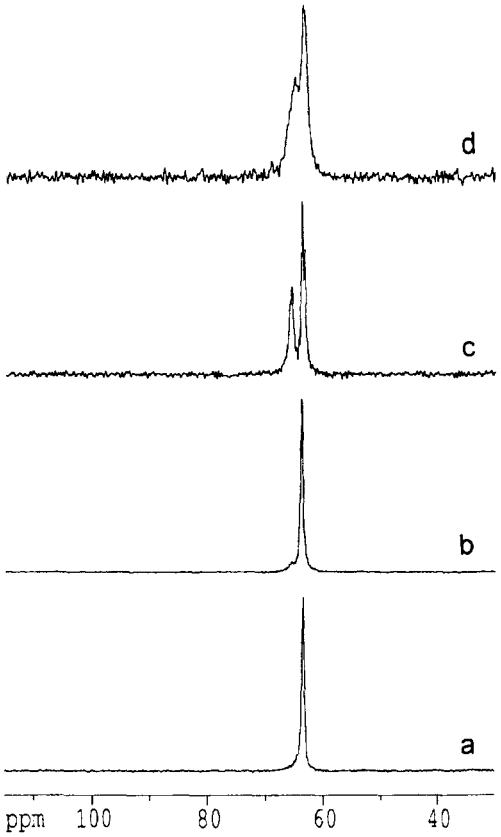

Fig. 11. ^{13}C MAS NMR spectra for (a) pure EG by HPDEC, (b) EG–silica dried at 50 °C by HPDEC, (c) by CP, (d) dried at 80 °C by HPDEC.

was used (b), while the spectrum measured by using the CP technique (c) showed quite different features. The peak at 65.6 ppm is assigned to methylene carbon in silicon glycoxide ($SiO-\underline{C}H_2CH_2OH$). The peak at around 63 ppm separated into two: A peak at 63.8 ppm is for free ethylene glycol, and that at 63.4 ppm is for an end methylene in silicon glycoxide. Furthermore, the S/N ratio of the spectra measured by CP became worse than that by HPDEC. Because carbons in elastic and fluid compounds are not detected by CP, the difference between spectra (b) and (c) suggests that a large portion of EG observed by HPDEC exists as a fluid in the gel dried at 50 °C, and that it is not detected by CP. The spectrum of the sample dried at 80 °C by HPDEC (d) was similar to that at 50 °C by CP (c), although the peaks became somewhat broader, because free EG was removed after drying at 80 °C for 48 h.

Figures 12, 13, and 14 show ^{13}C NMR spectra of dried gel containing DEG, TEG, and HEG, in turn. The assignments of the resonances in each pure organic compound are listed in Table 3. The spectra of DEG- and TEG-silica had essentially the same trend as the EG-silica: the spectra of gel dried at 50 °C by HPDEC and CP differed from each other, and that at 80 °C by HPDEC was similar to that at 50 °C by CP, while the peaks of samples dried at 80 °C became somewhat broader. On the contrary, for HEG-silica, the spectra of 50 °C samples by HPDEC and CP coincided

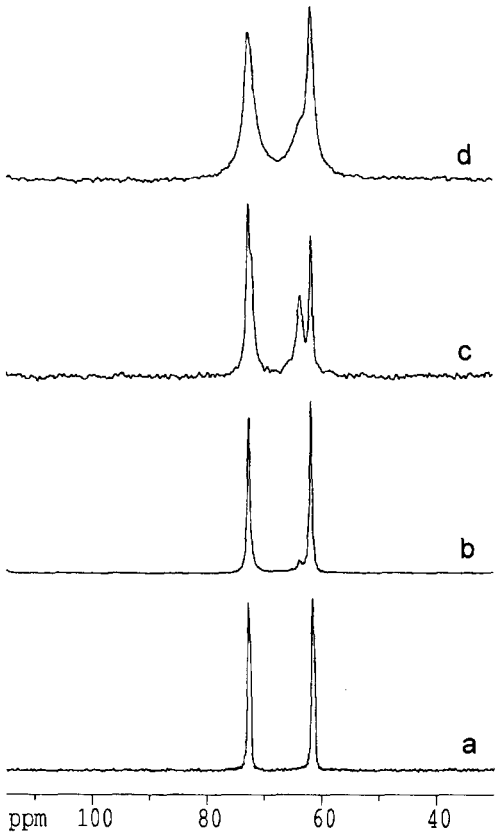

Fig. 12. ^{13}C MAS NMR spectra for (a) pure DEG by HPDEC, (b) DEG–silica dried at 50 °C by HPDEC, (c) by CP, (d) dried at 80 °C by HPDEC.

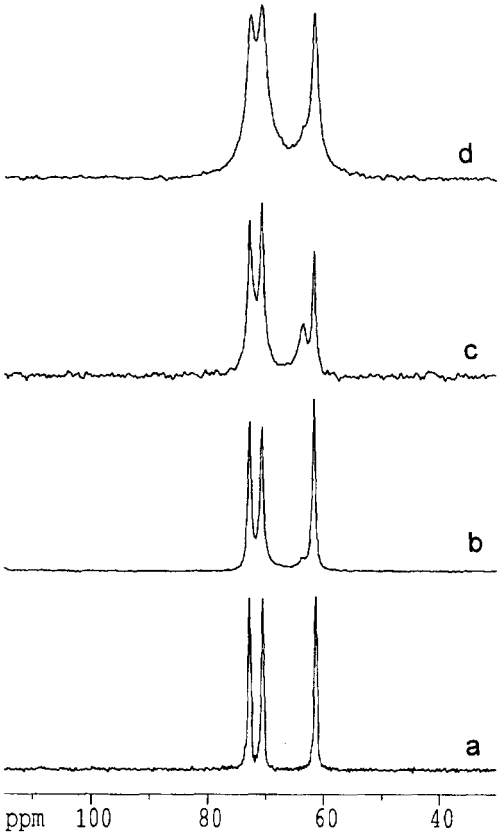

Fig. 13. ^{13}C MAS NMR spectra for (a) pure TEG by HPDEC, (b) TEG–silica dried at 50 °C by HPDEC, (c) by CP, (d) dried at 80 °C by HPDEC.

Table 3. Assignment of ^{13}C NMR Spectra of EG and Its Oligomers

EG	$HO\underline{C}H_2\underline{C}H_2OH$	63.8
DEG	$HO\underline{C}H_2\underline{C}H_2-O-\underline{C}H_2\underline{C}H_2OH$	61.8 72.8
TEG	$HO\underline{C}H_2\underline{C}H_2-O-\underline{C}H_2\underline{C}H_2-O-\underline{C}H_2\underline{C}H_2-OH$	61.8 72.9 70.8
HEG	$HO\underline{C}H_2\underline{C}H_2-O-(\underline{C}H_2\underline{C}H_2-O)_4-\underline{C}H_2\underline{C}H_2-OH$	61.7 72.7 70.7

with each other. Although the peaks became broader than those of pure HEG, the ratios of the intensities of the 3 peaks did not change. Namely, HEG was immobilized in silica gel unless $Si-(OCH_2CH_2)_nOH$ bonds were formed. A slight change was observed in the spectrum after being dried at 80 °C. Among these 4 composites from EG- to HEG-silica dried at 50 °C, the intensity of the peak at 66 ppm due to $Si-O\underline{C}H_2\underline{C}H_2O-$ decreased with increasing n, and the peak almost disappeared for HEG-silica when CP was used in the measurement.

In the measurement of SAXS, no scattering was detected from all dried samples.

Discussion

Interaction between Silica Network and PEG by Hydrogen Bond. In an investigation of phase separation in silica sol–gel systems containing organic polymers, Nakanishi et al. reported that the interaction between the organic polymer and the silica network plays an important role in phase relation.[15–18] When poly(acrylic acid) (HPAA) is used, the reacting solution separates into two phases, one rich in silica and the other rich in HPAA, because of decrease in entropy. Such a phase relation is commonly observed in a binary organic polymer solution.[29] On the other hand, a PEO-containing system shows a characteristic phase relation, in which polymerized silica and PEO become major constituents in one of the conjugate phases.[17] To account for the observation, they have proposed the existence of a strong attractive interaction between the PEO chain and the silica polymer due to hydrogen bonding between ether oxygen in PEO and silanol. Because the hydrogen bonding decreases the solubility of the PEO in the solvent, phase separation in the PEO–silica system takes place between solvent and the PEO associated with silica. One of the authors has shown that the interaction between PEO and silica arises before the onset of phase separation, and affects the polymerization process of silica species.[30] The interaction of PEO and silica also affects the evolution of the pore structure in xerogel during

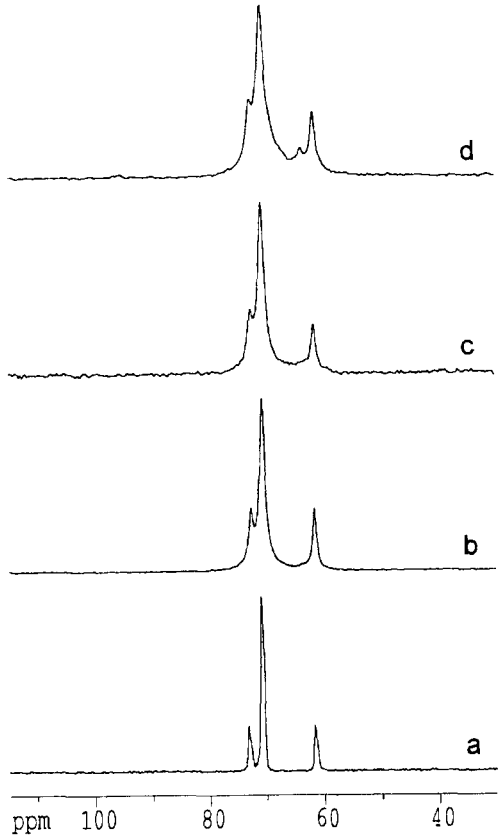

Fig. 14. ^{13}C MAS NMR spectra for (a) pure HEG by HPDEC, (b) HEG–silica dried at 50 °C by HPDEC, (c) by CP, (d) dried at 80 °C by HPDEC.

drying and heating.[21] Although phase separation does not take place at an average molecular weight of PEO less than 8000, Nakanishi et al. have suggested that a similar interaction arises between silica and PEO with a small molecular weight.[18]

Because PEO and PEG are composed of the same oxyethylene unit and differ only in molecular weight, PEG also interacts with the surface silanol of polycondensed silica through ether oxygen. In the ^{13}C MAS NMR of PEG3000–silica dried at 50 °C (Figs. 10b and 10c), a large peak of methylene carbon is observed which is sharper than that in pure PEG3000 (Fig. 10a). Namely, each methylene in the composite is in a similar chemical environment. As speculated in a preceding paper for PEO,[21] the PEG chain and the silica gel network would semi-interpenetrate each other, forming a large number of hydrogen bonds between silanol and the ether oxygen in PEG. Because the PEG chain distributes in the gel matrix randomly, the sharp peak is observed in the ^{13}C NMR spectrum.

Changes in the Interaction with Length of Poly(oxyethylene) Chain. In the HEG–silica, although HEG hardly interpenetrates with the silica-gel network, because of a shorter oxyethylene chain of HEG, we can assure from the ^{13}C NMR results that HEG also forms a hydrogen bond with silanol. Because pure HEG is fluid at room temperature, no resonance is observed for it by a CP measurement. The spectra of HEG–silica by HPDEC and CP coincide each other (Figs. 14b and 14c), and are similar to that of pure HEG by HPDEC (Fig. 14a), although the peaks become somewhat broader. The results suggest that the HEG molecules are attached onto the silica surface without forming covalent bonds, but probably forming hydrogen bonds. Lesot et al. have also suggested in an investigation of PEG with an average molecular weight of 200 in silica gel that part of PEG in the silica–PEG composite derived from sol–gel rote are solidified on silica by hydrogen bonds.[31] Among the ^{13}C NMR spectra of composites dried at 50 °C by CP (Figs. 10, 11, 12, 13, and 14c), the S/N ratio of the spectra by CP increased with increasing n. Thus, it can be said that the amount of additives solidified on silica increases with increasing n. These results also suggest that the strength of the interaction between silica and each oligoEG molecule through hydrogen bonds increases with increasing the length of the poly(oxyethylene) chain.

The interaction between additives and the silica-gel network affects the polymerization degree of silica in dried gel because the interaction between the PEG and silanol decreases the number of silanol available for polycondensation, and the PEG chain which interpenetrates with the silica-gel network inhibits the approach of silanol groups by shrinkage during drying. The decrease in the Q^4/Q^3 ratio with an increase in n (Table 2) also indicates that the interaction between PEG and silica and/or its effect on silica gel structure are enlarged with an increase in the length of the poly(oxyethylene) chain.

Here, we can consider two effects as being the reason why the strength of the interaction changes: a statistical one, and one caused by changes in the strength of each hydrogen bond with n. Although it is difficult to quantify the later contributions, we can well explain the experimental results only by a statistical consideration. Each hydrogen bond is much weaker than the usual covalent bond, and is easily broken. In DEG and TEG molecules, there are single and two ether oxygens in a molecule, respectively, while HEG has five, and PEG3000 has ca. 67 ether oxygens. If we count the end hydroxy group as a functional group forming hydrogen bond with silanol, the numbers are 3, 4, 7, and 69 for DEG, TEG, HEG, and PEG3000, respectively. Because of the large number of functional groups, HEG is attached on the silica-gel surface more strongly than TEG and DEG, and PEG3000 is attached more strongly than HEG. If we consider the additives eliminated exothermically in TG-DTA profiles (Figs. 6 and 7) as additives interacting with the silica-gel surface, the amount increases with n. The trend well agrees with the ^{13}C NMR results.

Esterification Reaction of Silanol with EG Oligomers. In addition to the hydrogen bond between the ether oxygen in PEG and silanol, an esterification reaction between silanol and the end OH group in the EG oligomer can not be ignored, particularly for EG and its oligomers with a shorter oxyethylene chain. In a pioneer work by Toba et al., they proposed eight kinds of possible structures in the bond formation between metal (Si or Al) and diol additives.[11]

Among them, however, we can ignore the coordinate bond, i.e. a bond type such as M–O(H)–R, where M is metal and R is alkyl, because Si can not remain coordination numbers larger than 4 under the usual sol–gel conditions. In the case of EG, therefore, the 3 types of bonding with Si shown in Chart 1 are considerable: Here, the extremely small Q^2 proportion in the ^{29}Si NMR spectrum (Fig. 8) suggests that the structure (A) is minor, if present. Furthermore, the ^{13}C NMR spectrum (Fig. 11c), the resonance assigned to $SiO\underline{C}H_2-$ is a single peak and the $HO\underline{C}H_2-$ resonance splits into 2 peaks, suggests that there are two kinds of EG which interact with silica: one forms glycoxide and the other is probably immobilized by hydrogen bonds; also, the major constituent by an esterification reaction between silanol and EG is (C). Thus, the present study clearly shows that EG does not act as a bidentate ligand of Si (A) nor as a bridging ligand of two Si atoms (B), as long as the sol-gel reaction takes place at room temperature.

In DEG and TEG, similar products to the monoester are also recognized in the ^{13}C NMR spectra (Figs. 12 and 13). However, their proportion steeply decreases with increasing n, probably due to a steric-hindrance effect of the long poly(oxyethylene) chain and/or a decrease in the number of free silanol sites by hydrogen bonds between the silanol and the ether oxygen in the poly(oxyethylene) chain. If we consider the number of additives forming a monoester as an index of the strength of the interaction between the silica gel network and the additives, the strength of interaction between the silica and the additives by ester formation decreases steeply with increasing n. Because the interaction by hydrogen bonding increases with increasing n, the overall strength of the interaction passes a minimum with a change in n, as illustrated in Fig. 15.

Key Role of PEG in Pore Formation. Because silicas obtained by the sol–gel method are essentially porous materials and their structure changes with different preparation conditions, it is difficult to specify the real effect of additives. Therefore, in order to clarify the effect of additives on pore formation, it is preferred that the gel be prepared under conditions in which xerogel without organic additives has no pores. In the preparation of microporous silica–zirconia using PEG, Yazawa et al. compared the dimension between PEG aggregates in water and the pore size of calcined gel, and suggested the templating effect of PEG on the pore structure of the resultant gel based on the similarity of both sizes.[13] According to them, the space occupied by PEG in the PEG–silica composite becomes pores after calcination. However, they obtained the pore size from the relation $d = 4v/s$, where d, v, and s are pore diameter, pore volume, and BET surface area, respectively. As described in the chapter of results, the BET surface area has no physical meaning for microporous materials because of micropore condensation. In addition, the structure of the PEG chain in-

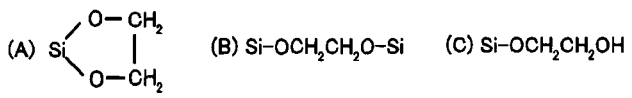

Chart 1.

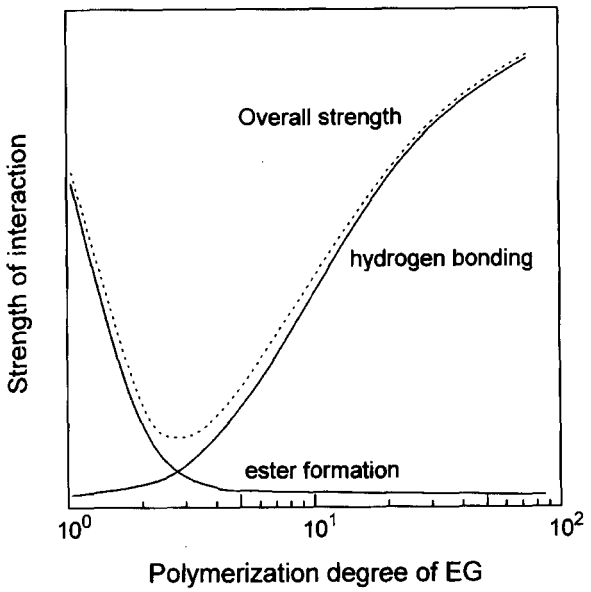

Fig. 15. Schematic drawing of changes in interaction between silica gel network and EG oligomers with the polymerization degree of oligomer.

corporated in silica gel is quite different from that in water because of the interaction with silanol through the hydrogen bond.[21] Thus, we must test whether the PEG acts as a simple template or not by an alternative means. One of the convenient procedure to test the problem is to compare the volume of pores in calcined samples with that occupied by organic compounds in organic–inorganic composites.[32] In case of PEG3000–silica in the present study, considering that the dried gel is composed of SiO_2 and PEG, and that there is neither a pore nor other compounds in dried samples, the volume occupied by PEG is obtained by dividing the PEG/SiO_2 weight ratio in the starting composition by the density of PEG. The volume becomes ca. 5-times larger than the pore volume in the calcined sample when we postulate the density of PEG to be 1 g cm^{-3}. Namely, the PEG–silica composites shrink much during calcination, probably together with the combustion of PEG. Thus, it is hardly considered that PEG acts as a simple template. The formation of micropores in the PEG–silica system is possibly attributed to the effect of PEG on the shrinkage behavior of silica gel during drying and heating.

The wet silica gel prepared under acidic conditions comprised a polymeric network rather than colloidal aggregates.[28] Such a polymeric gel shrinks homogeneously during drying, and any inhomogeneous portion in the network remains as an origin of micropores after sintering by heating.[33] In this work, the gel was prepared in an open container so that gelation would be accelerated by evaporation of the solvent, leading to a less crosslinked gel network. Thus, the dried gel showed no X-ray scattering, regardless of the addition of PEG or not. Because scattering in a small-angle range occurs when a sample has a structural correlation in the nm length scale, the data indicate that the distribution of Si in the dried gel was perfectly random. Usually, small clus-

ters, which are considered to link together by a percolation manner to be a gel, are formed during the initial stage of the sol–gel process.[28] Therefore, a scattering which corresponds to the structural correlation in these clusters is observed from the reacting solution, wet gel and xerogel. The observation that no scattering was recognized in the present dried gel suggests that the structural correlation in clusters formed during the initial stage of the sol–gel reaction disappeared by a deformation of the gel network and/or by additional Si–O–Si bond formation during the aging and drying. The disappearance of a structural correlation possibly occurs because the reacting solution turns to gel before the crosslinking density in cluster increases sufficiently. Thus, the dried gel has a random distribution of Si. Because of the homogeneity of dry gel, a gel with no organic additives shrinks uniformly, and have no pores after calcination at 500 °C.

The addition of PEG possibly changes the structural evolution manner in drying and heating by restricting the Si–O–Si bond formation. When the PEG, which hinders silanol from polycondensation, is removed at 210 °C by heating, abrupt Si–O–Si bond formation proceeds together with a collapse of the space which has been occupied by PEG. Concurrently, inhomogeneous domains will be formed by such abrupt condensation, and micropores remain after calcination. This is considered to be an origin of micropores in silica prepared from the PEG–silica system.

Effect of Sol–Gel Conditions on Micropore Formation. As described above, in addition to the differences in the condensation degree and aggregation manner of silica clusters in the sol–gel reaction, we speculate that the formation of a heterogeneous domain by abrupt Si–O–Si bonding during the combustion of PEG plays a key role in micropore formation. Based on this idea, we can explain the changes in the micropore volume based on the reaction conditions shown in Figs. 2 and 3. At a composition of $x = 0.37$, the molar ratio of oxyethylene unit (CH_2CH_2O) to Si is ca. 0.5, and volume occupied by PEG3000 is ca. 50 vol%. Because the amount of PEG3000, $x = 0.37$, is large enough to interact with the available silanol in dried gel, PEG3000 works well for micropore formation, even at that amount. An increase in the PEG3000 amount possibly causes an enhancement of the formation of inhomogeneous domains and retards thier sintering, because the density of the silica network in PEG3000-silica composite decreases with increasing it. When changing the H_2O/TEOS amount (R), the difference in the gelation time may affect the micropore volume. The gelation time in an open system is prolonged with an increase in the amount of solvent. This leads to a higher crosslinking density in silica clusters, so that a greater inhomogeneous portion is introduced to the silica gel network. Thus, the micropore volume gradually increases with increasing x (Fig. 2) and R (Fig. 3).

The polymerization degree of oligoEG (n) changes the strength of the interaction between the silica network and any additives. When an additive which shows a smaller interaction with silanol is used, silica gel possibly forms an additional Si–O–Si bond with less restriction in the composite, leading to less inhomogeneous domain formation after the combustion of additives. Therefore, the micropore volume decreases with decreasing n from PEG3000 to TEG (Fig. 4). In case of the addition of EG, an ester bond formed between EG and silanol also restricts the Si–O–Si bond formation during heating. In a similar manner to the PEG, Si–O–Si bonds are formed abruptly after removing EG, leading to the formation of micropores. Although the amount of EG bonded on the surface of silica gel is smaller than that of oligoEG (Figs. 6 and 7), EG works effectively for pore formation, because it combusts at a higher temperature. The higher condensation degree of silica in dry EG–silica than that in other oligoEG–silica, as shown in Fig. 8, is also considered to contribute to the formation of heterogeneous domains. Thus, the strength of interaction between the silanol and additives plays a key role in micropore formation. The changes in the micropore and the total pore volumes with n (Fig. 4) suggest that the minimum in the overall strength of the interaction between additives and silica locates at $n = 3$, i.e. at TEG (Fig. 15).

The difference in the interaction among organic additives is also said to result in the dependence of the micropore volume on pH of the reacting solution (Fig. 5). Since the esterification reaction is catalyzed by both acid and base, the number of EG bonded on silica changes with pH of the solution. Because the isoelectric point of the silica surface is ca. 2, the esterification reaction minimizes at pH = 2. The pH dependence of the micropore volume (Fig. 5), where the micropore volume is minimized at pH = 2 in EG, is accounted for in terms of the rate of the esterification reaction. In the TEG– and PEG3000–silica systems, on the other hand, because the interaction by hydrogen bonding between silanol and ether oxygen is dominant, the changes in the micropore volume with pH of the starting solution are smaller than that observed in the EG–silica system.

Conclusion

A mechanism for micropore formation in the sol–gel process in the presence of EG and its oligomers was investigated. There are two kinds of interactions between silica gel and organic additives in dried gel. At $n < 3$, bond formation between silanol and additives by esterification reaction is dominant, while hydrogen bonds between silanol and ether oxygen in additives are dominant at $n > 3$. These interactions restrict the condensation reaction forming Si–O–Si bonds during the drying and heating steps. When the organic additives are combusted, inhomogeneous domains, which are an origin of micropores, are formed by abrupt Si–O–Si bond formation. The stronger the interaction is, the larger does the pore volume of the micropores become. The number of ester bonds formed decreases, and the strength of the interaction due to hydrogen bonding increases with the increase in n. Because the combination of the interactions minimizes at an appropriate polymerization degree, a minimum in the micropore volume is observed at TEG.

Financial support by a Grant-in-Aid for Encouragement of

Young Scientists (No. 11750580) and "Research for the future" Program (JSPS-RFTF96P00304), both from the Japan Society for the Promotion of Science, are gratefully acknowledged. The authors wish to thank Prof. Kazuki Nakanishi, Department of Material Chemistry, Graduate School of Engineering, Kyoto University, for the use of SAXS apparatus.

References

1 R. S. A. de Lange, J. H. A. Hekkink, K. Keizer, and A. J. Burggraaf, *J. Non-Cryst. Solids*, **195**, 203 (1996).

2 P. B. Weisz and V. J. Frilette, *J. Phys. Chem.*, **64**, 382 (1960).

3 P. B. Weisz, *Stud. Surf. Sci. Catal.*, **7**, 3 (1981).

4 C. Lange, S. Storck, B. Tesche, and W. F. Maier, *J. Catal.*, **175**, 280 (1998).

5 M. Maeda, X. Wang, S. Tomura, F. Ohashi, M. Suzuki, and K. Okada, *J. Ceram. Soc. Jpn.*, **106**, 428 (1998).

6 K. Okada, H. Kawashima, Y. Saito, S. Hayashi, and A. Yasumori, *J. Mater. Chem.*, **5**, 1241 (1995).

7 W. G. Fahrenholtz, D. M. Smith, and D. W. Hua, *J. Non-Cryst. Solids*, **144**, 45 (1992).

8 W. G. Fahrenholtz and D. M. Smith, *Mater. Res. Soc. Symp. Proc.*, **271**, 705 (1992).

9 L. Chu, M. I. T.-Tejedor, and M. A. Anderson, *Mater. Res. Soc. Symp. Proc.*, **346**, 855 (1994).

10 Y. Lu, G. Z. Cao, P. P. Kale, L. Delattre, C. J. Brinker, and G. P. Lopez, *Mater. Res. Soc. Symp. Proc.*, **435**, 271 (1996).

11 M. Toba, S. Niwa, K. Shimizu, and F. Mizukami, *Nippon Kagaku Kaishi*, **1989**, 1523.

12 M. Toba, F. Mizukami, S. Niwa, and K. Maeda, *J. Chem. Soc., Chem. Commun.*, **1990**, 1211.

13 T. Yazawa, A. Miyake, and H. Tanaka, *J. Ceram. Soc. Jpn.*, **99**, 1094 (1991).

14 H. Izutsu, F. Mizukami, T. Sashida, K. Maeda, Y. Koizumi, and Y. Akiyama, *J. Non-Cryst. Solids*, **212**, 40 (1997).

15 K. Nakanishi and N. Soga, *J. Am. Ceram. Soc.*, **74**, 2518 (1991).

16 K. Nakanishi and N. Soga, *J. Non-Cryst. Solids.*, **139**, 1 (1992).

17 K. Nakanishi, H. Komura, R. Takahashi, and N. Soga, *Bull. Chem. Soc. Jpn.*, **67**, 1327 (1994).

18 K. Nakanishi and N. Soga, *Bull. Chem. Soc. Jpn.*, **70**, 587 (1997).

19 I. Langmuir, *J. Am. Chem. Soc.*, **40**, 1361 (1918).

20 B. C. Lippens and J. H. de Bore, *J. Catal.*, **4**, 319 (1965).

21 R. Takahashi, K. Nakanishi, and N. Soga, *Faraday Discuss.*, **101**, 249 (1995).

22 S. Brunauer, P. H. Emmett, and E. Teller, *J. Am. Chem. Soc.*, **60**, 309 (1938).

23 E. P. Barrett, L. S. Joyner, and P. P. Halenda, *J. Am. Chem. Soc.*, **73**, 373 (1951).

24 R. W. Cranston and F. A. Inkley, *Adv. Catal.*, **9**, 143 (1954).

25 D. Dollimore and G. R. Heal, *J. Appl. Chem.*, **14**, 109 (1964).

26 R. S. Mikhail, S. Brunauer, and E. E. J. Bodor, *J. Colloid Interface Sci.*, **26**, 45 (1968).

27 G. Horvath and K. Kawazoe, *J. Chem. Eng. Jpn.*, **16**, 470 (1983).

28 C. J. Brinker and G. W. Scherer, "Sol–Gel Science, The Physics and Chemistry of Sol–Gel Processing," Academic Press, New York (1990).

29 P. J. Flory, "Principles of Polymer Chemistry," Cornell University (1953).

30 R. Takahashi, K. Nakanishi, and N. Soga, *J. Sol–Gel Sci. Technol.*, **17**, 7 (2000).

31 P. Lesot, S. Chapuis, J. P. Bayle, J. Rault, E. Lafontaine, A. Campero, and P. Judeinstein, *J. Mater. Chem.*, **8**, 141 (1998).

32 R. Takahashi, S. Takenaka, S. Sato, T. Sodesawa, K. Ogura, and K. Nakanishi, *J. Chem. Soc., Faraday Trans.*, **94**, 3161 (1998).

33 R. Takahashi, K. Nakanishi, and N. Soga, *J. Non-Cryst. Solids*, **189**, 66 (1995).